J Appl Electrochem (2010) 40:561–573
DOI 10.1007/s10800-009-0029-6

ORIGINAL PAPER

Potentiometric determination of the chloride ion activity in cement based materials

Ueli Angst · Bernhard Elsener · Claus K. Larsen · Øystein Vennesland

Received: 6 July 2009 / Accepted: 25 September 2009 / Published online: 11 October 2009

Abstract The chloride content at the reinforcement is one of the decisive factors for the initiation and propagation of localised corrosion in concrete structures. A monitoring technique for the chloride concentration which is accurate, non-destructive and continuous would thus be highly desirable. For this reason, the performance of ion selective electrodes (ISEs) was investigated both in alkaline solutions and embedded in mortar. The Ag/AgCl electrodes used in this work showed Nernstian behaviour with a slope of –59 ± 1 mV per decade and a detection limit for chloride ions below 10^{-2} mol dm^{-3} even at pH close to 14; the selectivity coefficient for hydroxide interference was estimated at $k^{pot}_{Cl^-,OH^-} \approx 4 \cdot 10^{-3}$. The Ag/AgCl membranes show good long-term stability over more than 6 months even in highly alkaline solutions as long as chloride ions are present; in the complete absence of chloride the measured potentials were affected by the pH of the solution. The sensors are, however, able to recover fast as soon as they come into contact with chloride. When using ISEs embedded in concrete, diffusion potentials between the reference electrode and the ISE, as arising e.g. from gradients in pH, significantly affect the potential measurement and present a most important error source for the application of direct potentiometry to concrete. To minimise such errors, the reference electrode has to be positioned as close to the ISE as possible.

Keywords Ion selective electrode · Direct potentiometry · Membrane potential · Chloride induced corrosion · Reinforced concrete

U. Angst (✉) · C. K. Larsen · Ø. Vennesland
Department of Structural Engineering, NTNU Norwegian University of Science and Technology, Richard Birkelandsvei 1A, 7491 Trondheim, Norway
e-mail: ueli.angst@ntnu.no

B. Elsener
ETH Zurich, Institute for Building Materials (IfB), ETH Hönggerberg, 8093 Zurich, Switzerland

C. K. Larsen
Norwegian Public Roads Administration, 0033 Oslo, Norway

1 Introduction

With regard to chloride induced corrosion, both the process of chloride ingress into concrete, as well as the level required for corrosion initiation, the critical chloride content, are of great interest. In order to study these mechanisms, measurement of the chloride content in concrete is needed. This is normally done with well-established methods [1, 2] that yield the so-called total chloride content of the concrete and require destructive sampling (drilling, grinding, etc.). A non-destructive technique would not only be less time-consuming, but also allow continuous measurement of the chloride content. In this respect, attempts have been made to apply direct potentiometry to concrete. Ion selective electrodes (ISEs) are well established and have long been used in many fields such as analytical chemistry to determine the ionic activity of a certain species by a potential measurement. In concrete, experience with silver/silver chloride electrodes was gained in the 1980s by employing them as embeddable reference electrodes where they showed good long-term stability over a period of 4.5 years [3, 4]. The first documented attempt to measure chloride ion activities with Ag/AgCl electrodes in hardened mortar was reported in the early 1990s [5], and since, others have studied the performance of ISEs in simulated or real pore solutions [6–10], embedded in cement paste [11],

mortar [7, 10, 12–14] or concrete [15], or used them as chloride sensors in experiments on reinforcement corrosion in concrete [16–18]. Calibration curves following Nernst's law were reported for a wide range of chloride concentrations in alkaline media [5, 7–10, 12–14]. Some discrepancy can be noted regarding the long-term stability of the ISE [10, 12] that can be ascribed to different procedures of sensor fabrication [13].

The present article discusses the applicability of Ag/AgCl ISEs as a non-destructive chloride measurement technique in concrete. Theoretical considerations and experimental results show the feasibility and long-term stability of the sensors in principle, but also highlight error sources connected to the application of direct potentiometry in concrete.

2 Theoretical background

2.1 The silver/silver chloride electrode

The silver/silver chloride electrode is a solid-state membrane electrode that usually consists of a silver wire with a coating of silver chloride. As this salt coating has a low solubility, the electrolyte around the ISE is easily saturated with it and the potential of the electrode, $E_{Ag/AgCl}$, follows Nernst's law:

$$E_{Ag/AgCl} = E^{o}_{Ag/AgCl} - \frac{RT}{F} \ln a_{Cl^-}. \quad (1)$$

Here, R is the gas constant, F the Faraday constant, T the absolute temperature (K), and a_{Cl^-} the activity of the chloride ions in solution. $E^{o}_{Ag/AgCl}$ expresses the standard potential of the silver/silver chloride equilibrium reaction as follows:

$$E^{o}_{Ag/AgCl} = E^{o}_{Ag/Ag^+} + \frac{RT}{F} \ln K_S, \quad (2)$$

where E^{o}_{Ag/Ag^+} is the standard potential of the silver/silver ion electrode, and K_S the solubility product constant of AgCl, which can be found in tables such as [19].

2.2 Error sources in direct potentiometry

2.2.1 Interfering ions

The surfaces of solid-state membranes consisting of sparingly soluble salts are not only sensitive to the ions of the salt, but also to other species that tend to form precipitates of low solubility with a constituent ion; the AgCl membrane, for instance, responds to Ag^+, Cl^-, Br^-, I^-, OH^-, etc. [20, 21]. The selectivity of ISEs is based on the fact that they favour one primary species among several others. The interference of other ions is commonly taken into account by use of selectivity coefficients, $k^{pot}_{i,j}$ (with i standing for the primary and j for the interfering ions), and Eq. 1 is written in the following form, the so-called Nikolskij–Eisenman equation [21–23]:

$$E_{Ag/AgCl} = E^{o}_{Ag/AgCl} - \frac{RT}{F} \ln \left(a_{Cl^-} + \sum_j \left(k^{pot}_{Cl^-,j} \cdot a_j^{-1/z_j} \right) \right). \quad (3)$$

Here, a_j is the activity of the interferent and z_j its charge (which is a signed quantity).

In analytical applications, selectivity coefficients should be as close to zero as possible so that the electrode exhibits linear Nernstian behaviour over a large range. A chloride ISE deviates from this behaviour as soon as the relation

$$a_{Cl^-} \gg \sum_j \left(k^{pot}_{Cl^-,j} \cdot a_j^{-1/z_j} \right) \quad (4)$$

is not valid anymore. When the concentration of a certain interfering ion Y is sufficiently high, so that

$$a_{Cl^-} \ll k^{pot}_{Cl^-,Y} \cdot a_Y^{-1/z_Y}, \quad (5)$$

Equation 3 becomes independent of the activity of the primary ion, and the potential of the ISE depends on the activity of ion Y with a Nernstian slope [23]. The detection limit for the primary ion is located between the two characteristic ranges where conditions according to Eqs. 4 and 5, respectively, are met. A practical detection limit is graphically determined from the intersection of the extrapolated linear segments of a graph of ISE potential against the logarithm of the primary ion activity (Fig. 1) [24]. Analytically, this corresponds to $k^{pot}_{Cl^-,Y} \cdot a_Y^{-1/z_Y}$, which illustrates that the detection limit depends on the concentration of the interferent Y.

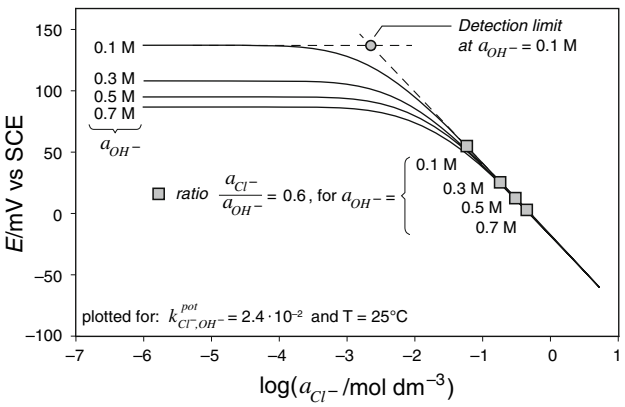

Fig. 1 Effect of hydroxide interference on the potential of the chloride ISE according to Nikolskij–Eisenman equation; plotted for various OH^- activities and a selectivity coefficient according to [25]

In concrete pore solution, many ions are present. The interferent of most practical importance are hydroxide ions, which are released in considerable amounts during cement hydration from $Ca(OH)_2$, KOH and NaOH. The selectivity coefficient for OH^- as the interferent for an Ag/AgCl electrode has been reported to be $k^{pot}_{Cl^-,OH^-} = 2.4 \cdot 10^{-2}$ [25]. Based on this value, the effect of hydroxide interference can be estimated for a certain pH: For instance, at a typical OH^- concentration of ca. 0.5 M the limit of chloride ion detection would be around 10^{-2} mol dm^{-3}. At such high pH values, however, the activity of hydroxide ions will be lower than the concentration, which gives a somewhat lower (better) detection limit. This has been plotted in Fig. 1, where four different activities of OH^- ions in the range of typical concrete pore solutions were assumed. When the activity of the interferent decreases, the point of deviation from linearity is shifted towards smaller chloride concentrations.

With regard to chloride induced corrosion, it might be the ratio of chloride to hydroxide ions that is of more importance than the chloride concentration alone. If as a rough estimate, a threshold value of $Cl^-/OH^- = 0.6$ [26] is considered, the interfering hydroxide ions are present in slight excess over the chloride ions at the level where corrosion initiation is expected. It is then desirable that the selectivity coefficient $k^{pot}_{Cl^-,OH^-}$ is low enough so that Eq. 4 is fulfilled. Figure 1 shows that the chosen critical chloride to hydroxide ratio of 0.6 is in the linear section of Eq. 3 at all pH values. Hydroxide interference is thus not significant at such chloride concentrations.

If seawater is the chloride source, other ions are also present and might affect the potential response of chloride ISEs by interference. In this regard, bromide has been reported to depress the electrode potential even at low concentrations as is the case in seawater [15, 27]. This would lead to overestimation of the chloride concentration.

2.2.2 Activity versus concentration

The conversion from chloride activity into chloride concentration is a basic difficulty with potentiometric measurements. It is occasionally assumed that concentration and activity is the same, which, to a first approximation, is true in dilute solutions, but in highly alkaline solutions the high ionic strength causes larger differences between activity and concentration. This can be taken into account by using activity coefficients. Table 1 shows a selection of values for mean activity coefficients of sodium chloride, $\gamma_{\pm}$, in aqueous solution [19, 28, 29]; particular activity coefficients of the chloride ion, γ_{Cl^-}, in synthetic pore solutions have been measured experimentally by use of a chloride ISE and calculated with a theoretical model [8]; in addition, attempts have been made to determine γ_{Cl^-} in pore solutions expressed from Portland cement pastes (pH 13.08–13.53) [9]. The activity coefficient appears to be in the range 0.5–0.8 for most situations relevant for practice. Thus, if this is neglected when converting from activity to concentration, concentrations determined with chloride ISE will deviate from values obtained with e.g. titration techniques by a factor of 1.3–2.

In this context, it is also worth mentioning that for chemical analysis of expressed pore solution, the obtained sample is usually diluted. This affects the activities of all ions present in the solution. Accurate back-calculation is difficult, since the ionic strength of the solution and chloride activity coefficients do not change proportionally during dilution [5].

2.2.3 Stability at high pH

The stability of the chloride ISE in highly alkaline solutions must be ensured; otherwise, the application in concrete pore solution is not feasible. It was observed by some authors that the potential of the silver/silver chloride electrode decreased with time when immersed in solutions of high pH and in simultaneous absence of chloride [10, 12]. This was attributed to damage of the ISE membrane by formation of silver oxides [10] or silver hydroxide [13].

In the presence of hydroxide ions, the AgCl membrane can undergo metathesis and become partially covered with AgOH. This reaction can only take place at sufficiently low chloride concentrations, namely if the following condition is fulfilled [22]:

$$\frac{K_S(AgCl)}{K_S(AgOH)} > \frac{a_{Cl^-}}{a_{OH^-}}. \quad (6)$$

Elsener et al. [13] calculated that at hydroxide concentrations of typical concrete pore solutions an AgOH layer might be formed below chloride concentrations of ca. 0.002 mol dm^{-3}. However, silver hydroxide is unstable and tends to convert to argentous oxide, Ag_2O, according to the reaction $2AgOH \rightleftarrows Ag_2O + H_2O$ [30]. An electrode membrane consisting of both AgCl and Ag_2O would exhibit a mixed potential, determined by the two possible chemical equilibriums: the Ag/AgCl electrode acts as a chloride ISE as discussed above, whereas the Ag/Ag_2O electrode is sensitive to hydroxide ions (pH sensor). The potential response of the latter also follows Nernst's law:

$$E_{Ag/Ag_2O} = E^o_{Ag/Ag_2O} - \frac{RT}{F} \ln a_{OH^-}. \quad (7)$$

The standard electrode potential, E^o_{Ag/Ag_2O}, can be estimated at ca. 344 mV SHE from solubility product constants K_S at 25 °C of the reaction $Ag_2O + H_2O \rightleftarrows 2Ag^+ + 2OH^-$ [30]. If the membrane is considered to be completely covered with Ag_2O, the electrode would exhibit a potential solely

Table 1 Mean activity coefficients for NaCl ($\gamma_{\pm}$) and activity coefficients of the chloride ion (γ_{Cl^-}) (at 25 °C)

Chloride ion concentration (molal)									Remarks	Ref.
0.001	0.01	0.02	0.1	0.2	0.5	1.0	2.0	3.0		
0.965	0.903	0.952	0.779	0.734	0.681	0.657	0.668	–	$\gamma_{\pm}$ for NaCl in aqueous solution	[19]
0.965	0.903	–	0.778	0.735	0.681	0.657	–	0.714	$\gamma_{\pm}$ for NaCl in aqueous solution	[28]
0.965	0.902	0.871	0.778	0.734	0.682	0.658	0.671	0.720	$\gamma_{\pm}$ for NaCl in aqueous solution	[29]
–	0.74	–	0.61	0.59	0.57	0.55	0.54	–	γ_{Cl^-} experimentally determined in 0.5 m KOH + sat. $Ca(OH)_2$	[8]
–	0.638	–	0.627	0.618	0.597	0.579	0.568	–	γ_{Cl^-} calculated for 0.5 m KOH and 0.5 m KOH + sat. $Ca(OH)_2$	[8]
–	–	–	1.41	1.10	0.45	0.42	0.41	–	γ_{Cl^-} experimentally determined in expressed pore solutions	[9]
0.666	0.663	–	0.656	0.652	0.631	0.604	0.578	–	γ_{Cl^-} calculated for expressed pore solutions	[9]

determined by Eq. 7; at pH 14, it would take on the value of E^{o}_{Ag/Ag_2O}. Švegl et al. [10] found experimentally that Ag/AgCl electrodes in chloride free, alkaline sodium hydroxide solutions exhibited lower potentials when the pH was above 12, and approached the value of E^{o}_{Ag/Ag_2O} at pH 14.

2.2.4 Temperature

The potentials of both the chloride ISE and the reference electrode, E_{RE}, against which the measurement is performed, depend on temperature. The measured potential can be written as follows (by including conversion from natural to base-10-logarithm):

$$E_m = E^{o}_{Ag/AgCl} - \frac{RT}{F \log e} \log a_{Cl^-} - E_{RE}. \quad (8)$$

When a silver/silver chloride electrode is used as reference electrode, and both the reference electrode and chloride ISE have the same temperature, then $E^{o}_{Ag/AgCl}$ is eliminated and temperature only affects RT/*F*. In case of another reference electrode, proper values for $E^{o}_{Ag/AgCl}$ and E_{RE} have to be used, which are available in the literature for a wide range of temperatures [28, 29, 31].

Parameters for Eq. 8 are presented in Table 2 for temperatures between 15 and 30 °C together with the potentials of the saturated calomel electrode (SCE), which is a commonly used reference electrode. $E^{o}_{Ag/AgCl}$ and SCE have similar temperature coefficients of ca.−0.6 to −0.65 mV °C^{-1} [28, 29, 31], and thus the error is comparatively small when the complete measuring chain according to Eq. 8 is considered, as is apparent from the last column in Table 2.

For the special case of a temperature difference between the ISE and the reference electrode, Atkins et al. [15] demonstrated that already small temperature differences can lead to significant errors.

Table 2 Parameters of the Nernst equation for the chloride ISE and sat. calomel reference electrode (without liquid junction) at selected temperatures, given in mV, according to ref. [28, 29, 31]

T (°C)	$E^{o}_{Ag/AgCl}$	2.303 RT/*F*	E_{SCE}	$E^{o}_{Ag/AgCl} - E_{SCE}$
15	228.5	57.17	247.7	−19.2
20	225.6	58.16	244.5	−18.9
25	222.4	59.16	241.2	−18.8
30	219.2	61.15	237.9	−18.7

2.2.5 Measuring through concrete

Apart from errors related to the ISE itself, measurement of the correct potential is crucial for reliable determination of the chloride concentration since direct potentiometry is highly sensitive to variations in potential; even small variations in the range of a few millivolts adversely affect the accuracy of this chloride quantification technique [21]. When applying ISEs in concrete, several phenomena might disturb the measurement of the correct sensor potential [32]. The reason for this is that reference and ISEs are normally located at different positions. If the measurement path is in the field lines of e.g. macrocell corrosion, the iR drop affects the potential reading. In the case of concentration gradients within the concrete, e.g. differences in pH, membrane potentials are established and present a significant error source for the measurement of the ISE potential [32, 33].

3 Experimental

3.1 Sensor element

The chloride ion sensitive electrodes (chloride sensors) used in this work consist of a silver wire coated with silver chloride (chloride deposited by anodising). The tip, which

Table 3 Calibration solutions and corresponding liquid junction potentials (mV) in the SCE frit

Chloride concentration (mol dm^{-3})	Calculated liquid junction potential $E_{junction}$ (at 25 °C)		
	Dist. water	Sat. $Ca(OH)_2$	Synthetic pore solution
0.002	−3.77	−1.55	–
0.01	−2.94	−1.46	3.58
0.1	−1.50	−0.81	3.65
0.5	0.14	0.52	3.96
1.0	1.19	1.48	4.32
2.0	2.55	2.75	–
3.0	3.50	3.67	5.55

is the exposed electrode surface, was in addition dipped in an AgCl melt in order to achieve a more stable membrane. The ISEs were produced by a manufacturer of commercial reference electrodes.

3.2 Calibration in solution

The chloride sensors were calibrated in distilled water, saturated calcium hydroxide and synthetic pore solution consisting of 0.2 M KOH + 0.15 M NaOH + sat. $Ca(OH)_2$. The solutions contained known concentrations of sodium chloride ranging from 0.002–3.0 mol dm^{-3}. The electrode potentials were measured versus a SCE immersed into the same solution at a temperature of 20–21 °C. After each measurement, the chloride sensors were rinsed with distilled water and carefully dried before immersion into the next solution; for comparison, some sensors were not cleaned between the experiments. It was found that this does not affect the final value of the stable potential but can influence the response time.

Liquid junction potentials, $E_{junction}$, established across the interface between the reference electrode (SCE) and the calibration solution were calculated by use of the Henderson equation [20]. The solutions used and the calculated liquid junction potentials are presented in Table 3. For the calculations, it was assumed that KCl is saturated at 4.16 mol dm^{-3} and $Ca(OH)_2$ at 0.011 mol dm^{-3} (at room temperature). The measured potentials, E_m, were corrected with regard to liquid junction potential errors and calibration curves were obtained by linear regression analysis according to the following equation:

$$E = E_m - E_{junction} = m \cdot \log a_{Cl^-} + b. \quad (9)$$

The differences between chloride activity and concentration were taken into account by using mean activity coefficients for sodium chloride, $\gamma_{\pm}$, according to Table 1.

3.3 Calibration in mortar

Cylindrical mortar samples 20 mm in diameter and 70 mm in length with a centrally embedded chloride sensor were cast with two different w/c ratios (0.4 and 0.6). After hardening during almost 2 months, the samples were immersed in synthetic pore solution (0.2 M KOH + 0.15 M NaOH + sat. $Ca(OH)_2$) containing three different concentrations of sodium chloride: 0.1, 0.3 and 0.5 M. Three parallel mortar samples of each *w/c* ratio were exposed to each solution. For comparison, chloride sensors, which had been dipped in cement paste and were thus covered with a thin cement paste layer, as well as blank chloride sensors, were also kept in the solutions (three parallel sensors each). The sensor potentials were periodically measured versus a SCE that was placed in the solution for the duration of the measurement (10–20 min). The exposure solutions were regularly checked with regard to chloride concentration and pH and renewed when necessary. The temperature was 20–22 °C throughout the whole experiment. After a total immersion time of 9 months, immersion was terminated and the samples were split in order to remove the embedded ISEs. Pore solution was pressed out of the three parallel samples together at a pressure of 280 MPa. As the sample volume was rather small, this was only possible in the case of $w/c = 0.6$ and even then, pressure had to be applied during up to 1 h in order to obtain enough pore liquid. Chloride concentrations were subsequently analysed in the pressed out pore solution by a spectrophotometric method. Further experimental details are given in reference [34].

3.4 Long-term stability

Chloride sensors were immersed in solutions of various alkalinity and chloride concentrations during more than 6 months. The potential of the electrodes was periodically recorded versus a SCE that was immersed into the solution for the measurement. For every solution, three parallel sensors were fixed in plastic bottles, which could be closed in order to avoid carbonation of the exposure solutions. The composition of the solutions is presented in Table 4. After 6 months, some selected sensors were removed and examined with the scanning electron microscope (SEM) equipped with energy-dispersive spectrometers (EDS).

4 Results and discussion

4.1 Calibration in solution

The results of the calibration measurements and the linear regression analysis according to Eq. 9 are given in Table 5

Table 4 Solutions used to study the long-term stability of chloride sensors

KOH (mol dm^{-3})	NaCl (mol dm^{-3})	Mean activity coefficient $\gamma_{\pm}$ for KOH [19]	Approximate pH	Solution colour owing to immersion of sensors
0.0001	0	~1	10.0	Transparent
0.01	0	0.9	12.0	Yellowish
	0.1			Transparent
	0.5			Transparent
0.1	0	0.8	12.9	Blackish
	0.1			Transparent
	0.5			Transparent
1.0	0	0.7	13.9	Blackish
	0.1			Blackish
	0.5			Slightly blackish

Table 5 Parameters of calibration curves obtained from linear regression analysis

Solution	m (mV/decade)	b (mV)	R^2
Distilled water	−58.3	−16.8	0.9999
Sat. $Ca(OH)_2$	−57.6	−17.3	0.9998
Synthetic pore solution	−57.8	−19.3	0.9990
Theoretical (20 °C)	−58.2	−18.9	

for all three solutions. Figure 2 shows the calibration curve obtained in synthetic pore solution before and after correcting the measured potential, E_m. It is apparent that the values used for correction, i.e. mean activity coefficients, $\gamma_{\pm}$, and theoretical liquid junction potentials, $E_{junction}$, lead to excellent agreement between the calibration results and the theoretical curve. Also given in Fig. 2 are the standard deviations of the potential readings obtained from five parallel sensors that were in addition used several times (measurements repeated). The scatter between chloride sensors increases with decreasing chloride concentration in the solution; at a low concentration of 0.1 M NaCl the difference between the smallest and the largest potential value was 3 mV (on a basis of ten measured values). The generally small deviations from Nernstian behaviour are also reflected in the coefficients of determination R^2 (Table 5).

The calibration curve depicted in Fig. 2, which was obtained in synthetic pore solution with a hydroxide ion concentration larger than 0.35 M, does not show any signs of deviation from linearity even at the lowest chloride concentrations. For comparison, the curve in Fig. 1 starts deviating from linearity in the range 0.1–0.01 M chloride activity at similar hydroxide concentrations. This implies that the selectivity coefficient for hydroxide interference, $k^{pot}_{Cl^-,OH^-}$, is lower than the value of $2.4 \cdot 10^{-2}$ [25], which was assumed to plot Fig. 1. Thus, the chloride ISEs used in

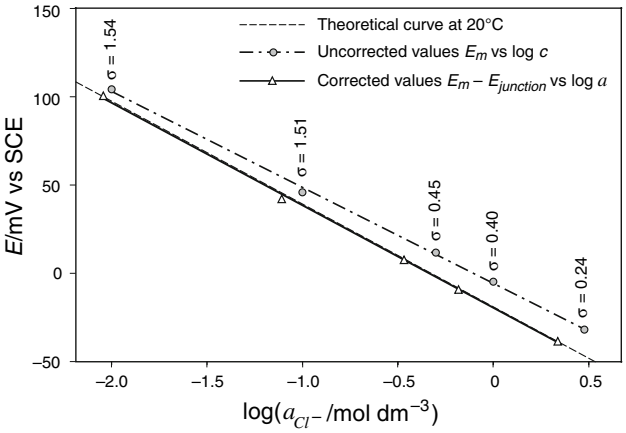

Fig. 2 Calibration curve of chloride sensors in synthetic pore solution (mean values and corresponding line fit by linear regression analysis)

the present work appear to have a lower chloride detection limit and show less pronounced hydroxide ion interference.

4.2 Calibration in mortar

Figure 3 depicts the potentials of blank, paste covered and embedded chloride sensors during immersion in synthetic pore solution. Only the results obtained for exposure to 0.3 M sodium chloride are presented here; those measured in 0.1 M and 0.5 M NaCl give a similar picture. Note that the measured values, E_m, were directly plotted without correcting for liquid junction potentials at the SCE/solution interface.

The potentials of the embedded sensors decrease steadily as chloride solution penetrates the mortar, the process being faster in the more porous samples with $w/c = 0.6$. The blank sensors and those covered with a thin layer of cement paste are rather stable near the corresponding equilibrium potential, with a trend towards lower potentials, especially after ca. 40 days. At about the same time,

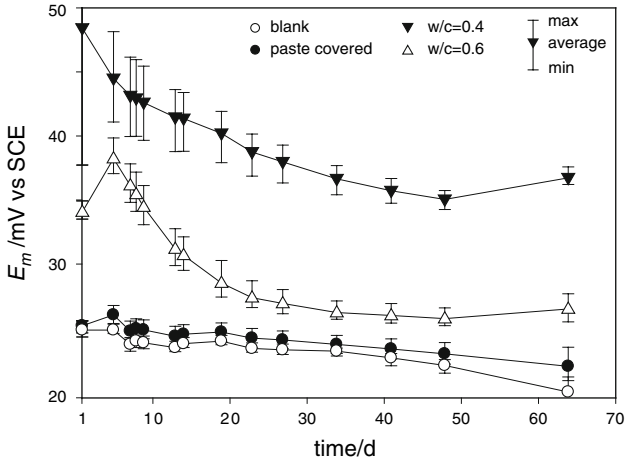

Fig. 3 Sensor potentials during immersion in synthetic pore solution with 0.3 M NaCl (*circles* represent the blank and cement paste covered sensors; *triangles* represent the sensors embedded in cylindrical mortar samples) [34]

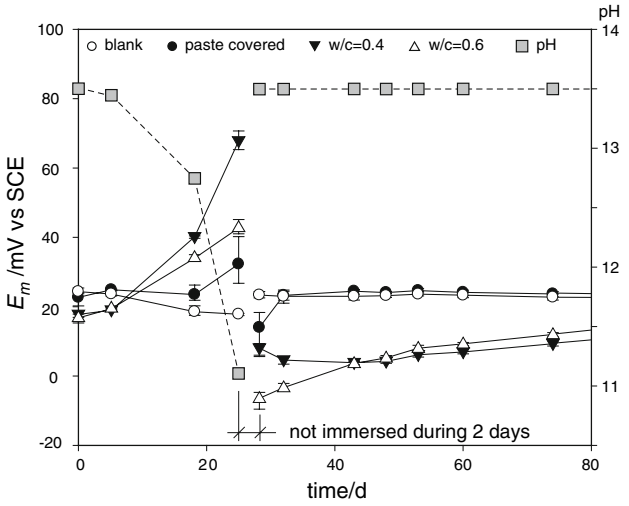

Fig. 4 Sensor potentials after renewal of the exposure solution and measured pH during phases with and without prevention of carbonation; immersion in synthetic pore solution with 0.3 M NaCl [34]

the potentials of the embedded sensors appear to increase instead of falling continuously. A possible explanation for these deviations from the expected behaviour is carbonation of the exposure solution [34]: a decrease in pH over time raises the chloride activity, which is reflected by lower potentials of those sensors that are directly in contact with the exposure solution. The observed potential increase in the case of embedded sensors, on the other hand, is owing to diffusion potentials that are established as the result of pH gradients (compare Sect. 2.2.5): whereas the pH decreases in the exposure solution, it is still high in the mortar sample due to buffering by hydration products and thus a pH gradient is present along the measuring path. As a result, a positive diffusion potential is established, i.e. the measured potential is higher than the true potential of the embedded sensor.

Figure 4 shows two later phases where carbonation was provoked by exposing the solution constantly to CO_2-bearing air, and prevented by keeping the complete setup in a controlled CO_2-free environment [34]. Again, only the results from exposure to 0.3 M sodium chloride are presented; those measured in 0.1 M and 0.5 M NaCl show the same phenomena. The solutions were renewed before both phases and the pH was periodically checked with a glass electrode as well as with pH indicator papers. The obtained values depicted in Fig. 4 clearly illustrate carbonation during the first phase and a stable solution pH in the second phase. While the pH is falling from initially 13.5 towards 11, the potentials of the embedded sensors increase markedly, and those of the blank sensors show a trend towards less positive potentials as discussed above. As soon as the solution is renewed, the blank sensor potentials jump back to the original value, whereas those of the embedded sensors immediately drop to a clearly lower level. This can be interpreted in the following way: after renewing the solution, the pH is higher in the exposure solution than inside the mortar samples. As a result of this inversion of the pH gradient, the associated diffusion potentials have a negative sign and thus lead to lower potential readings. This explanation is supported by the fact that diffusion potentials are established fast, whereas changes at the embedded chloride sensors would require comparatively slow mass transport through the mortar.

The time axis in Fig. 4 ends at 80 days, but data was measured until t = ca. 150 days. This corresponds to 4 months uninterrupted immersion in non-carbonating solution. After that, all the potentials had flattened out on a certain level. This implies the following hypotheses.

(i) All concentration gradients between sample and external solution have levelled out, and accordingly, no diffusion potentials are present anymore.
(ii) There are still concentration differences, but they are constant (steady-state) and thus, the associated diffusion potentials are constant over time (e.g. when considering buffering of the internal pore solution and a constant, lower pH in the external solution).

After that, immersion was terminated and pore solution was expressed for supplementary chloride analysis. Table 6 shows the last measured potentials, $E_{m,end}$, as well as their transformation into chloride concentrations by correcting for liquid junction potentials at the SCE, $E_{junction}$, and activity coefficients as described in Sects. 3.2 and 4.1. Also the chloride concentrations analysed in the expressed pore solution are given.

Note that the blank sensors directly immersed in the storage solutions are in good agreement with the concentrations

specified for each solution. The concentrations obtained from the embedded sensors, on the other hand, are ca. 25–70% higher than the external solution concentrations. They are, however, in good agreement with the chloride concentrations measured in the expressed pore solution, which are also higher than those in the storage solutions. It has been reported in the literature that, owing to the pressure applied during pore solution expression, part of the bound chlorides is released [35–37]. This might be true also in the present case, especially when considering the relatively long duration during which pressure was applied, and, as a result, the likely temperature increase in the sample. In addition, a minor contribution might be the exposure of the samples to CO_2-bearing air during handling, and associated drying or carbonation, which both increase the free chloride concentration.

The chloride concentrations in the pressed out pore liquid are in surprisingly good agreement with those obtained from the embedded chloride sensors (with a relative error $\leq 5\%$). When assuming that condition (ii) as described above is true, it could be reasoned that the diffusion potential error is, by coincidence, just as large to lead to the same increase in chloride concentration as the one caused by the applied pressure during pore solution expression. Accordingly, the higher concentrations in mortar, when measured with embedded ISEs or pore solution expression, would in both cases be owing to errors inherent to the measurement techniques. As a contrary view, hypothesis (i) implies that the measured sensor potential is true. In this case, to explain the concentration difference between external bulk solution and internal pore solution, it could be proposed that a chloride ISE not only responds to the chlorides freely dissolved in the pore solution, but also to part of the adsorbed chlorides, and that both these are also detected in solution obtained from pore solution expression due to the mentioned effects of applied pressure. This view, however, would involve a discussion on the various mechanisms of chloride binding and is outside the scope of the present article. Having in mind the size of the pores in concrete, another, not unlikely explanation would be the interaction between double layers and dissolved ions, which might affect the activity coefficient, thereby probably resulting in a higher chloride ion activity as when compared with bulk solutions. Certainly, more research is needed with regard to this.

It is worth mentioning that, when preparing the mortar samples for pore solution expression, the sensors were removed from the mortar and checked in two solutions of known chloride concentration. Even after having been embedded in mortar for ca. 11 months, the potential responses were in excellent agreement with those observed with "new" sensors.

4.3 Discussion of influence of diffusion potentials

The results shown in Fig. 4 can be analysed further: in a plot of measured sensor potential, E_m, versus pH in the exposure solution, the slope $\Delta E/\Delta pH$ would correspond to the membrane potential that is established per pH unit. This was done for the results obtained from exposure to 0.1, 0.3, and 0.5 M sodium chloride and is depicted in Fig. 5. As visible on the graph, the slope decreases with decreasing pH, i.e. the diffusion potentials established per pH unit are lower at lower pH values. This is in agreement with theoretical considerations [32], since at lower pH values, the chlorides that are present in solution become more dominating and limit the effect of pH changes. In addition, Fig. 5 shows that the slope $\Delta E/\Delta pH$ is generally lower in the case of $w/c = 0.6$ and also decreases faster when the solution carbonates than in the case of $w/c = 0.4$. This might be owing to the faster chloride ingress in the more porous mortar, leading to a higher internal chloride concentration. Another possible reason might be the less

Table 6 Potentials of blank and embedded chloride sensors at the end of immersion in different chloride solutions and corresponding chloride concentrations, $c_{Cl^-,ISE}$, calculated with the theoretical calibration curve at 20 °C, as well as chloride concentrations obtained from pore solution expression, $c_{Cl^-,expr}$

Synthetic pore solution	Sensor	$E_{m,end}$ (mV)	$E_{junction}$ (mV)	a_{Cl^-} (mol dm^{-3})	$\gamma_\pm$	$c_{Cl^-,ISE}$ (mol dm^{-3})	% Error $c_{Cl^-,ISE}$ vs. ext. solution	$c_{Cl^-,expr}$ (mol dm^{-3})	% Error $c_{Cl^-,ISE}$ vs. $c_{Cl^-,expr}$
0.1 M NaCl	Blank	45 ± 1	3.7	0.09	0.78	0.12	20	–	
	$w/c = 0.4$	39 ± 2	3.7	0.12	0.78	0.15	52	–	
	$w/c = 0.6$	36 ± 2	3.7	0.13	0.78	0.17	69	0.16	−5
0.3 M NaCl	Blank	23 ± 1	3.8	0.22	0.72	0.31	3	–	
	$w/c = 0.4$	14 ± 2	3.8	0.32	0.72	0.44	47	–	
	$w/c = 0.6$	17 ± 1	3.8	0.28	0.72	0.39	31	0.41	3
0.5 M NaCl	Blank	10 ± 1	4.0	0.37	0.68	0.55	10	–	
	$w/c = 0.4$	2 ± 2	4.0	0.51	0.68	0.75	50	–	
	$w/c = 0.6$	7 ± 3	4.0	0.43	0.68	0.63	26	0.65	3

pronounced permselective properties of cement paste at higher *w/c* ratios, as will be discussed below.

In order to illustrate the phenomenon of diffusion potentials and how it affects the use of embedded chloride sensors, a theoretical model as the one in reference [33] is useful. Diffusion potentials become an error source when the electrolyte in direct vicinity of the ISE has a different chemical composition than the electrolyte around the reference electrode. If both these compositions are known, and under the assumption of a linear concentration gradient, the diffusion potential can be calculated by the Henderson equation [20]. This equation describes diffusion potentials as a function of ionic mobility (or diffusivity), concentration, and charge of all the involved ions. In a nano-porous system such as mortar or concrete, the diffusivity of ions is affected by the so-called permselective properties of cement paste, namely in such a way that the difference in mobility between anions and cations becomes larger in cement paste compared with bulk solution [38–41]. When modelling diffusion potentials, these permselective properties of cement paste can thus be taken into account by modifying the ionic mobility of the involved ions. For the present model, the following ionic mobilities, u_i ($cm^2\ s^{-1}\ V^{-1}$), were used, as estimated from diffusivities measured in cement paste and reported in the literature [38–40]: $u_{Cl^-} = 1.5 \cdot 10^{-6}$ and $u_{Na^+} = u_{K^+} = 2.0 \cdot 10^{-7}$. The ratio u_{OH^-}/u_{Cl^-} was assumed to be 10 and thus $u_{OH^-} = 1.5 \cdot 10^{-5}$. In addition, the pore solution was assumed to consist only of sodium and potassium hydroxide. More information on this theoretical model can be found in reference [33].

The model is compared with experimental data in the following manner: the potential drops observed for the embedded chloride sensors after renewal of the carbonated exposure solution at $t \approx 25$ days in Fig. 4 were plotted for the three different chloride solutions in Fig. 6. In addition, theoretical membrane potentials were calculated as described above for all the chloride exposure solutions using the pH values measured before and after solution renewal, and by assuming that the chloride concentration has reached a constant concentration inside the mortar sample, corresponding to the one in the external solution. As apparent from Fig. 6, the calculated values are generally in good agreement with the measured ones. This indicates that both the application of the Henderson equation and the assumed ionic mobility values lead to reasonable results, although the Henderson equation is based on assumptions that are not rigorously fulfilled in the case of ionic transport through concrete [33]. Figure 6 also shows diffusion potentials calculated by using tabulated ionic mobilities valid for bulk solutions (pure NaOH or KOH). The fact that these are clearly lower than the measured values confirms the permselective properties of cement paste and illustrates that membrane potentials arising from internal concentration gradients in concrete are larger than they would be in bulk solutions. It was mentioned in the literature [39, 41] that the permselective properties of cement paste are a function of the *w/c* ratio: With increasing *w/c* ratio, diffusivities in cement paste increase towards their values in bulk solution, and also the differences in diffusivity between cations and anions become smaller. This was also observed in the present measurements, since the membrane potentials in mortar with $w/c = 0.4$ are always higher than those in the more porous mortar samples (Fig. 6). In addition, the increase in membrane potential with decreasing NaCl concentration is more pronounced. Also this is in agreement with theory.

To sum up, a theoretical model based on the presence of diffusion potentials (calculated by the Henderson equation) is suitable to explain the variations of measured ISE

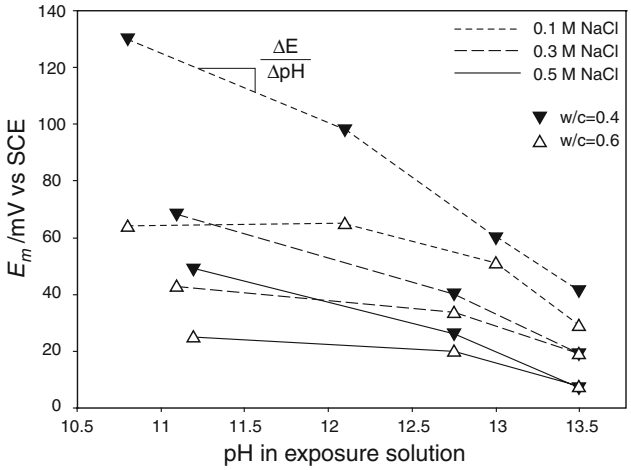

Fig. 5 Potentials of embedded sensors versus pH during carbonation of the external solutions

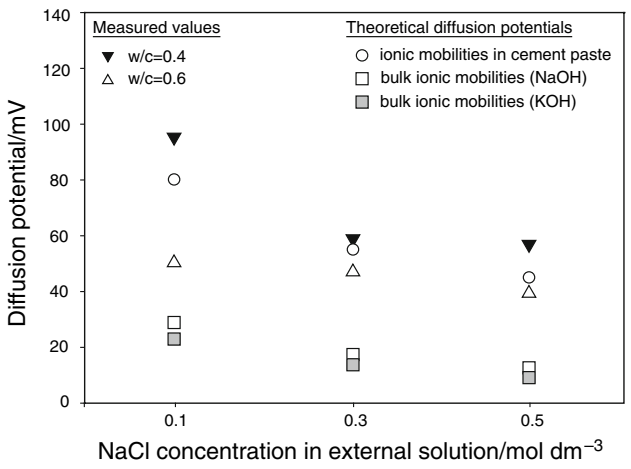

Fig. 6 Measured and calculated diffusion potentials established upon renewal of carbonated storage solutions

potentials observed in the experiments. The adverse effect of such membrane potentials is primarily governed by pH gradients, but also depends on chloride concentrations and permselective properties of the concrete. To be more precise, membrane potentials arising from pH gradients decrease with increasing chloride concentrations (as long as the chlorides are evenly distributed and do not exhibit concentration gradients themselves), and become larger in cement pastes with lower *w/c* ratios.

4.4 Long-term stability

Figure 7 shows the potentials of the sensors immersed in various alkaline solutions versus time as described in Sect. 3.4. In the presence of chloride, the potentials are stable over the complete exposure time even at high pH, varying by only ±1.5 mV. The scatter between the three parallel sensors is in the same range. Even after more than 6 months immersion, the potentials are still in good agreement with those obtained in the calibration measurements. The same result was reported by Elsener et al. [13] who used identical sensors embedded in mortar. In the absence of chloride, however, the potentials appear to be dependent on pH, being generally lower with increasing solution alkalinity. At the same time, they are less stable compared with those in chloride containing solutions and decrease monotonously over time. Whereas this is most pronounced during the first months, the values are more stable towards later stages, falling by less than 1 mV per week. In this context, it must be remembered that the relation between chloride activity and potential is logarithmic, i.e. at chloride concentrations close to zero the potential varies strongly even with minimal variations in chloride concentration.

By plotting the sensor potentials versus the logarithm of the chloride ion activity, as depicted in Fig. 8, it becomes apparent that the slopes between 0.1 and 0.5 M NaCl, calculated from average values over more than 6 months, are very close to the theoretical value of –58.16 mV/decade (at 20 °C). In the solutions that were prepared without any sodium chloride, the chloride concentration is very low, but not zero owing to the solubility of silver chloride of the ISE: from the solubility product of AgCl [19], a chloride concentration of $\sqrt{K_S} = 1.3 \cdot 10^{-5}$ mol dm^{-3} can be expected. At this concentration, the potentials of the sensors in the corresponding solutions were also plotted in Fig. 8, thereby presenting the initial potentials and those measured at the end of the experiments separately. If it is assumed that there is strong hydroxide ion interference in this range, and that the membrane of the ISE is initially unchanged in chemical composition, then the measured values can be compared to Fig. 1 as follows: By interpolating between the observed potentials, it becomes apparent that the curves in Fig. 8 would flatten out on higher potentials than the corresponding curves in Fig. 1; for instance, the dashed curve at 1 M KOH in Fig. 8 flattens out at ca. 130 mV SCE, and can be compared with the curve in Fig. 1 plotted for $a_{OH^-} = 0.7$ (by assuming an activity coefficient of 0.7 for 1 M KOH [19]) which levels out at ca. 85 mV SCE. Thus, the chloride sensors used in the present work show less pronounced interference from hydroxide ions than assumed in Fig. 1. From Eq. 3, it can be estimated that the actual selectivity coefficient for hydroxide interference, $k^{pot}_{Cl^-,OH^-}$, would be ca. $4 \cdot 10^{-3}$ and thereby almost one order of magnitude lower than the value reported in reference [25].

From theoretical considerations, as presented in Sect. 2.2.3, it might however be expected that at high pH values,

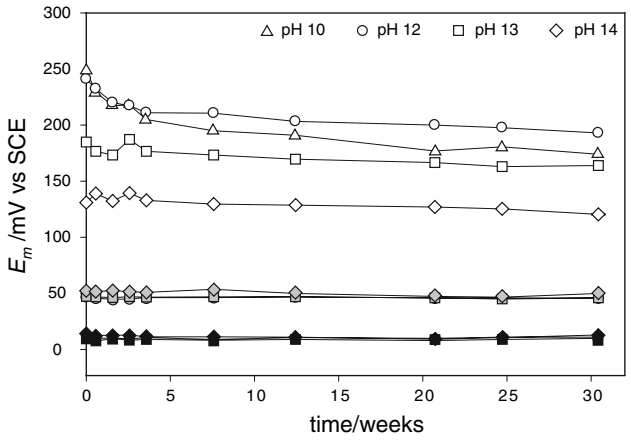

Fig. 7 Long-term stability: Average potential of three parallel sensors in solutions of various pH and chloride concentration versus time (*white symbols* = initially no chlorides; *grey symbols* = 0.1 M NaCl; *dark symbols* = 0.5 M NaCl)

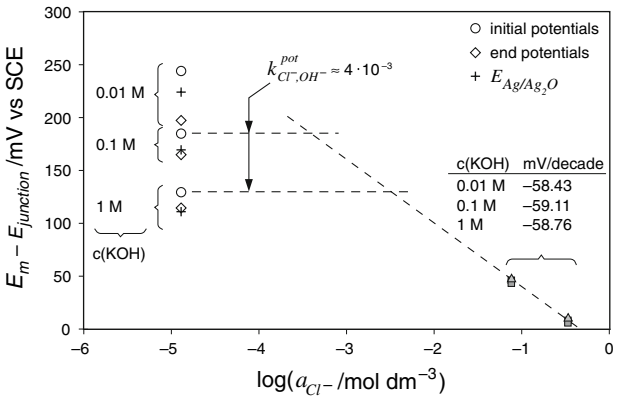

Fig. 8 Sensor potentials versus chloride ion activity during immersion over more than 6 months (average over time in the case of 0.1 and 0.5 M NaCl; for the chloride free solution the initial and end values are plotted separately)

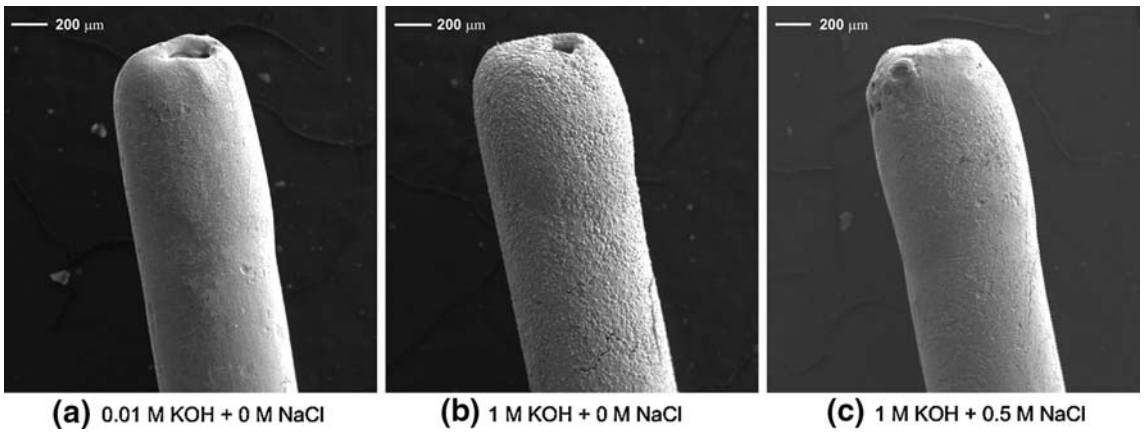

Fig. 9 SEM micrographs of the ISE membranes after more than 6 months immersion in various alkaline solutions. The topography appears to be dependent of both pH and chloride content in the solution

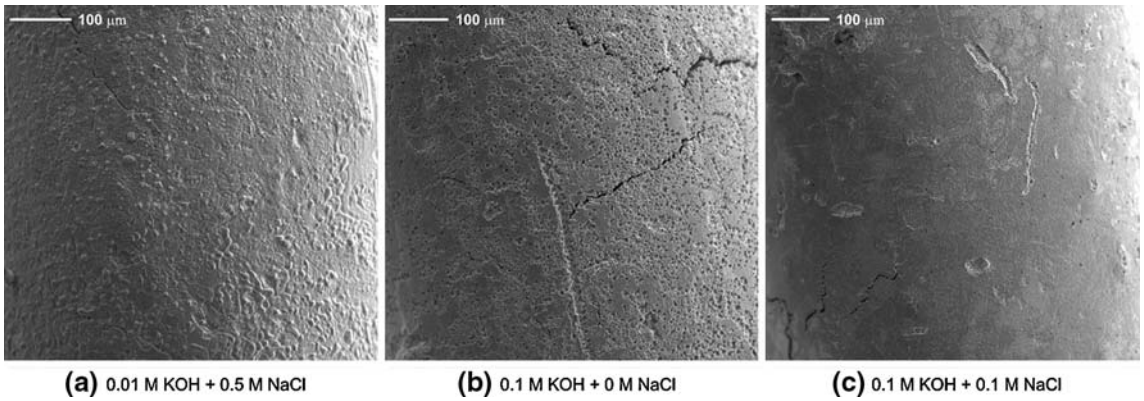

Fig. 10 SEM micrographs of the ISE membranes after more than 6 months immersion in various alkaline solutions. Small defects at the surface (detached particles) in the absence of chloride at pH $\approx$ 13 visible in **b**)

the AgCl membrane becomes unstable and is, partly or completely, turned into Ag_2O. In the case of complete transformation of the AgCl surface into Ag_2O, the electrode potential would be determined by Eq. 7, and assume the value $E_{Ag/Ag_2O} = 224$ mV SCE at $c(OH^-) = 0.01$ M, 169 mV SCE at $c(OH^-) = 0.1$ M, or 111 mV SCE at $c(OH^-) = 1$ M (calculated for 25 °C and assuming activity coefficients according to Table 4). When plotting these potentials for the Ag/Ag_2O electrode also in Fig. 8, it becomes apparent that in the case of 0.1 and 1 M KOH, the end potentials of the chloride sensors are close to E_{Ag/Ag_2O}, thereby implying that the electrode surface is continuously transformed into Ag_2O and thus acts as a pH sensor rather than a chloride sensor. In 0.01 M KOH, on the other hand, the potentials decreased to clearly lower values than the corresponding E_{Ag/Ag_2O}.

In order to study the uncertainties with regard to chemical transformation of silver chloride in the presence of high hydroxide ion concentrations, microanalysis of selected sensors was carried out. Figure 9 shows scanning electron micrographs from selected sensor tips after more than 6 months of constant immersion. Apparently, the surface morphology of electrodes that were exposed to moderately alkaline (ca. pH 12) solutions, even in the absence of chloride ions (Fig. 9a), and electrodes exposed to a highly alkaline (ca. pH 14), but chloride containing solution (Fig. 9c), are very similar. Electrodes immersed at pH close to 14 and in the absence of chloride ions, on the other hand, exhibit a clearly rougher surface topography (Fig. 9b). Higher magnifications of selected sensor surfaces, as depicted in Fig. 10, confirm that the surface morphology appears to depend on the alkalinity and chloride concentration of the exposure solution. In the case of pH ca. 13 and in the absence of chloride (Fig. 10b), small defects are visible on the surface, giving the impression of detached particles; this was not observed at the same or lower pH and when chloride ions were present (Fig. 10a, c). It might be speculated that, as soon as the condition described in Eq. 6 is fulfilled, silver oxides or hydroxides can form, but they do not necessarily adhere to the membrane surface. In this context, it might also be worth mentioning that the initially transparent immersion solutions assumed different colours

with time, as given in the last column of Table 4. Whereas the ions Ag^+ and Cl^- themselves are colourless, the compounds AgO and Ag_2O are grey-black and brown-black, respectively [42].

Energy-dispersive spectrometry with a sampling depth of ca. 500 nm did not indicate the presence of oxide. Thus, the membrane, when examined with EDS, appears to consist purely of silver chloride.

It was finally observed that the sensors recover fast as soon as they come into contact with chloride: the sensors were removed from immersion in chloride-free, alkaline solutions after more than 6 months and instead placed in solutions of corresponding alkalinity, but containing 0.5 M sodium chloride. In the case of 0.01 and 0.1 M KOH they responded to the chloride concentration correctly almost immediately; in the case of 1 M KOH, the sensors assumed the proper equilibrium potential within a few hours. Thus, it can be concluded that an eventual formation of silver oxide is fully reversible.

4.5 Additional remarks on the application of ISEs to concrete

When ISEs are embedded in concrete they are in direct contact with aggregates, cement paste and electrolyte solution. Some parts of the electrode surface might be screened from the electrolyte as the result of deposition of cement hydration products; in these areas, electrochemical reactions are likely to be restricted. The "active part" of the ISE would be those areas where the membrane is in direct contact with the concrete pore solution, i.e. directly adjacent to filled pores. Pore sizes in concrete vary from a few nanometres (gel pores) up to several millimetres (macro pores). As demonstrated above, ions behave differently in the pore solution in cement paste than in bulk solution. The mechanisms responsible for this phenomenon include physical and chemical adsorption, as well as double layer effects. In the present article, these permselective properties have only been addressed from an empirical point of view and it is outside the scope to investigate the detailed mechanisms more fundamentally. The effect of these phenomena on the activity of the chloride ions in the pore system of cement paste, a_{Cl^-}, i.e. the variable of interest, is at present unknown. It can, however, be expected that the influence is most pronounced in those areas of the ISE membrane that are in contact with the finest pores; in larger pores the relative importance of the double layer decreases and the pore solution might behave more like bulk solution.

It was shown above that the pH of the concrete pore solution can affect the potential of the ISE, especially by interference of hydroxide ions and by depressing the potential in the complete absence of chloride ions. The composition of the pore solution depends in the first place on the cement type: the amount of soluble alkalis in the cement determines the concentration of KOH and NaOH released during hydration and thus affects the alkalinity [43]. Also replacement of Portland cement by pozzolanic and mineral additions such as fly ash, silica fume, or blast furnace slag affects the pore solution composition, mainly by decreasing the pH [43].

From an engineering point of view, it might be useful to express the measured chloride content by concrete volume or weight, especially when comparing the chloride content in the pore solution with the total chloride content. For such a conversion, the amount of pore solution per concrete volume (or weight) is required. This would typically be obtained from the amount of pores per concrete volume combined with an assumption on the degree of saturation. In this regard, the *w*/*c* ratio and the age (degree of hydration) are important since the porosity of the cement paste is mainly dependent on these factors. It might be worth mentioning that the use of mineral additions also affects the pore size distribution of the paste.

5 Conclusions

From theoretical considerations as well as experiments on the application of ISEs as chloride sensors in concrete, the following conclusions can be drawn.

1. Ag/AgCl electrodes can be successfully used to measure the chloride ion activity in highly alkaline environments such as concrete. The detection limit for chloride ions in the presence of interfering hydroxide ions is below 10^{-2} mol dm^{-3} even at pH close to 14. In addition, the Ag/AgCl membranes show good long-term stability in highly alkaline solutions. Only in the complete absence of chloride the potential is influenced by pH; the sensors are, however, able to recover fast as soon as they come into contact with chloride.
2. When using ISEs embedded in concrete, the most critical step is measuring the correct potential. Membrane potentials between the reference electrode and the ISE arithmetically add to the true sensor potential and lead to erroneous potential readings. Having in mind the sensitivity of potentiometry towards potential variations, the presence of diffusion potentials along the measuring path has been identified as a most critical error source for the application of direct potentiometry to concrete. To minimise such errors, the reference electrode has to be positioned as close to the ISE as possible.
3. The sensors measure the activity of the free chloride ions. In a nano-porous system such as cement paste, the activity of dissolved chloride ions might be affected by double layer effects, physical adsorption and the

chemical equilibrium between bound and free chloride ions. It is thus not clear to which part of chlorides embedded ISEs respond. More research is required in this regard.

Acknowledgements The work described in this article forms part of the Norwegian COIN project (www.sintef.no/coin).

References

1. Recommendation of RILEM TC 178-TMC (2002) Mater Struct 35:583
2. ASTM C-1152. Standard test method for acid-soluble chloride in mortar and concrete. American Society for Testing and Materials
3. Geoghegan MP, Das SC (1986) UK Patent Application, No. 8429046, Taylor Woodrow Construction Limited, UK
4. Gurusamy KN, Geoghegan MP (1990) In: 3rd International symposium on corrosion of reinforcement in concrete, Wishaw, UK. Society of chemical industry, London, pp 333–347
5. Molina M (1993) Zerstörungsfreie Erfassung der gelösten Chloride im Beton. Diss. ETH Nr. 10315. ETH Zürich, Switzerland
6. Atkins CP, Scantlebury JD (1995) J Corros Sci Eng 1: Paper 2
7. Elsener B, Zimmermann L, Flückiger D et al (1997) In: Proceedings of RILEM international workshop on chloride penetration into concrete, Paris
8. de Vera G, Hidalgo A, Climent MA et al (2000) J Am Ceram Soc 83:640
9. Hidalgo A, de Vera G, Climent MA et al (2001) J Am Ceram Soc 84:3008
10. Švegl F, Kalcher K, Grosse-Eschedor YJ et al (2006) Rare Met Mater Eng 35:232
11. Atkins CP, Scantlebury JD, Nedwell PJ et al (1996) Cem Concr Res 26:319
12. Climent-Llorca MA, Viqueira-Pérez E, López-Atalaya MM (1996) Cem Concr Res 26:1157
13. Elsener B, Zimmermann L, Böhni H (2003) Mater Corros 54:440
14. Montemor MF, Alves JH, Simoes AM et al (2006) Cem Concr Compos 28:233
15. Atkins CP, Carter MA, Scantlebury JD (2001) Cem Concr Res 31:1207
16. Zimmermann L (2000) Korrosionsinitiierender Chloridgehalt von Stahl in Beton. Diss. ETH Nr. 13870. ETH Zürich, Switzerland
17. Elsener B, Angst U (2007) Corros Sci 49:4504
18. Schiegg Y, Böhni H (2000) Beton und Stahlbetonbau 95:92
19. Handbook of chemistry and physics (2007–2008), 88th edn, CRC Press, Boca Raton
20. Bard AJ, Faulkner LR (2001) Electrochemical methods. Fundamentals and applications, 2nd edn. Wiley, New York
21. Koryta J (1972) Anal Chim Acta 61:329
22. Janata J (1989) Principles of chemical sensors. Plenum Press, New York
23. Koryta J, Štulík K (1983) Ion-selective electrodes, 2nd edn. Cambridge University Press, Cambridge
24. Recommendations for nomenclature of ion-selective electrodes (1976) Pure Appl Chem 48:129
25. Umezawa Y (ed) (1990) CRC handbook of ion-selective electrodes: selectivity coefficients. CRC Press, Boca Raton
26. Hausmann DA (1967) Mater Protect 6:19
27. Junsomboon J, Jakmunee J (2008) Talanta 76:365
28. Shreir LL, Jarman RA, Burstein GT (1994) Corrosion, vol 2, 3rd edn. Butterworth Heinemann, Oxford
29. Dobos D (1975) Electrochemical data. A handbook for electrochemists in industry and universities. Elsevier Scientific Publishing Company, Amsterdam
30. Biedermann G, Sillén LG (1960) Acta Chem Scand 14:717
31. Ives DJG, Janz GJ (1961) Reference electrodes—theory and practice. Academic Press, New York
32. Angst U, Vennesland Ø, Myrdal R (2009) Mater Struct 42:365
33. Angst U, Vennesland Ø (2009) Mater Corros 60:638
34. Angst U, Larsen CK, Vennesland Ø et al. (2009) In: 3rd international conference on concrete repair "Concrete Solutions". Taylor & Francis, London, pp 401–405
35. Tritthart J (1989) Cem Concr Res 19:586
36. Glass GK, Wang Y, Buenfeld NR (1996) Cem Concr Res 26:1443
37. Larsen CK (1998) Dr. Ing. Thesis, Report No 1998:101. Norwegian University of Science and Technology
38. Goto S, Roy DM (1981) Cem Concr Res 11:751
39. Page CL, Short NR, El Tarras A (1981) Cem Concr Res 11:395
40. Chatterji S (1994) Cem Concr Res 24:1229
41. Atkinson A, Nickerson AK (1984) J Mater Sci 19:3068
42. Pourbaix M (1974) Atlas of electrochemical equilibria in aqueous solutions. Centre Belge d'Etude de la Corrosion CEBELCOR
43. Bensted J, Barnes P (eds) (2002) Structure and performance of cements, 2nd edn. Spon Press, London